Hippocampal Spreading Depression Bilaterally Activates the Caudal Trigeminal Nucleus in Rodents

Phillip E. Kunkler[1] and **Richard P. Kraig**[1,2,*]

[1]Department of Neurology, University of Chicago, Chicago, Illinois

[2]Department of Neurobiology, Pharmacology, and Physiology, University of Chicago, Chicago, Illinois

Abstract

Spreading depression (SD) and migraine aura involve transiently altered (i.e., increased followed by decreased) electrophysiological activity that propagates at the distinctive rate of millimeters per minute (mm/min), leading to the suggestion that they (and perhaps pain from migraine) are causally related via changes in the same brain structure. Neocortex is considered the anatomical zone associated with migraine aura and is the sole area known to induce caudal trigeminal nucleus (TNC) activation from SD in rodents. However, classical evidence of SD in human neocortex is reported only with severe brain disease, while migraine is a common and comparatively benign disorder. Because SD occurs in human hippocampus, and memory dysfunction referable to hippocampus is seen in migraineurs, we determined whether recurrent SD confined to hippocampus in rat could induce TNC activation. Our work shows that recurrent hippocampal SD evoked a significant ($P <$ 0.05–0.001) increase in bilateral c-*fos* immunostaining within TNC superficial laminae compared with sham controls. Furthermore, hippocampal SD occurred with a correlated and transient change in spontaneous activity and blood flow in the ipsilateral neocortex without spread of SD to that area. Thus, hippocampal SD may be a previously unrecognized, potential trigger for nociceptive activation of TNC perhaps associated with migraine.

Keywords

migraine; Fos protein; headache, aura; blood flow

INTRODUCTION

Migraine aura (Milner, 1958; Olesen et al., 1981, 1990; Andersen et al., 1988; Friberg et al., 1994; Lauritzen, 1994; Woods et al., 1994; Welch et al., 1998; Cao et al., 1999; Hadjikhani et al., 2001; James et al., 2001) may result from neocortical spreading depression (SD). Evidence of this potential interrelation stems from aspects of the classical defining characteristics of SD and how they might relate to the typical features of migraine aura through altered neocortical function. For example, SD consists of a propagating wave of electrical silence that travels through susceptible gray matter at millimeters per minute (mm/min) (Leão, 1944). By mapping the spread of his own migraine scotoma across primary visual neocortex, Lashley (1941) concluded that if the loss was generated there, it would travel at a rate of mm/min. Later, Milner (1958) suggested that such a loss of visual function might be due to the electrical silence of

*Correspondence to: Department of Neurology, MC 2030, University of Chicago, 5841 South Maryland Avenue, Chicago, IL 60637. rkraig@neurology.bsd.uchicago.edu.

SD. Grafstein (1956), and later Sugaya et al. (1975), noted that SD could occur with a transient increase in excitability. Thus, SD might also account for the increased functional activity, e.g., visual obscurations, often seen at the leading edge of a spreading scotoma from migraine (Lashley, 1941).

Numerous neuroimaging studies in humans, although never demonstrating classical defining characteristics of SD, provide inferential evidence that SD-like phenomena in neocortex occur with migraine aura (Olesen et al., 1981,1990;Andersen et al., 1988;Friberg et al., 1994;Lauritzen, 1994;Woods et al., 1994;Welch et al., 1998;Cao et al., 1999;Hadjikhani et al., 2001;James et al., 2001). The most recent is perhaps the most convincing of these studies. Hadjikhani et al. (2001) show that neocortical SD-like changes occur with visual aura in migraine patients. Using functional magnetic resonance imaging (MRI), these workers show slowly propagating neurovascular changes in visual cortex that were concomitant with visual symptoms of three patients who suffer from migraine with visual aura.

Neocortical SD also might account for the pain associated with migraine (Moskowitz et al., 1993). Neocortical SD in rodents can trigger ipsilateral increased activation of the superficial laminae of the trigeminal nucleus caudalis (TNC), a brainstem region that processes nociceptive information (Menetrey and Basbaum, 1987) via meningeal trigeminovascular sensory fiber afferents (Mayberg et al., 1981, 1984). This, in part, provided the comparatively direct evidence for the suggestion by Moskowitz and Macfarlane (1993) that SD might trigger migraine pain. However, while migraine is common (Ferrari, 1998), SD as defined by classical electrophysiological criteria, i.e., (1) slowly propagating (2) wave of electrical silence associated with (3) a large, negative interstitial DC change (Leão, 1944; Marshall, 1959; Bureš et al., 1974), has been extraordinarily difficult to elicit or detect in human neocortex.

SD is a robust perturbation that can alter brain function remote from the region experiencing SD. For example, recurrent neocortical SD triggers increased glial fibrillary acidic protein (GFAP) expression in neocortex and at least a synapse away in ipsilateral basal ganglia (Kraig et al., 1991). Furthermore, neocortical SD can trigger increased cyclooxygenase 2 expression at least four synapses away in brain structures that do not experience SD (Caggiano et al., 1996). Importantly, neocortical SD transiently alters spontaneous electrophysiological activity in the contralateral neocortical layer IV (Caggiano et al., 1996), where commissural fibers connect intercerebral hemisphere pathways (Cajal, 1995) without an associated, large negative interstitial DC change in that area.

Since altered neural circuit function can be seen remote from SD, we wondered whether neocortical SD is the sole brain area capable of triggering SD-induced activation of TNC or whether hippocampal SD could also evoke such nociceptive activation (i.e., as might be expected with migraine pain). The rationale for this focus to the hippocampus stemmed from several facts. First, hippocampus is the most sensitive mammalian brain region for SD (Bureš et al., 1974). Second, SD occurs in human hippocampus both in vitro (Avoli et al., 1991) and in vivo (Šramka et al., 1977/78). Third, the hippocampus has relatively direct and important functional interactions with brain regions likely to be important to migraine, e.g., those associated with emotions, neuroendocrine homeostasis, and vision (Cutrer et al., 2001). Fourth, meningeal TNC C-fiber afferents are most concentrated at the base of the brain, including around the hippocampus (Moskowitz, 1990). Fifth, migraineurs suffer interictal memory dysfunction that is referable to the hippocampus (Calandre et al., 2002). Our results show for the first time that hippocampal SD is a robust stimulus for bilateral nociceptive activation of the TNC. Aspects of this work were presented in preliminary form (Kraig and Kunkler, 1997).

MATERIALS AND METHODS

Animal Preparation and Recording

All surgical procedures were done under aseptic technique in accordance with the Institutional Animal Care and Use Committee. Wistar male rats (250–300 g; Harlan Sprague-Dawley, Indianapolis, IN) (n = 35) were prepared, using inhalational halothane, as previously described (Moskowitz et al., 1993), except as noted below. Two small (1.5-mm-diameter) craniotomies were drilled, leaving the dura intact at both sites after a left parasagittal scalp incision (Fig. 1). The more rostral site, used for recordings, was 2 mm caudal to bregma and 1.5 mm lateral to the midline. The more caudal site, used for KCl microinjections, was 6 mm caudal to bregma and 4.5 mm lateral to the midline. Bupivacaine was injected subcutaneously (0.1 ml), and the wound was closed with sterile 4/0 interrupted nylon sutures. Animals then were returned to their cages and kept normothermic until they awoke. During the ensuing 24 h, animals were allowed access to water but fasted overnight before being reanesthetized for electrophysiological recordings.

When deeply reanesthetized, a tail artery was cannulated for the sampling of arterial blood, pressure and glucose. Bupivacaine was reinjected (0.1 ml) into the wound edges; the cranial sutures were removed 5 min later. In an effort to minimize noxious facial stimulation, the head was placed in a mold of plaster, fitted with soft foam rubber, instead of a stereotactic frame (Strassman et al., 1994). Eye drops (Murine Tears™) were placed in both eyes to retard corneal drying and associated activation of TNC (Strassman and Vos, 1993). The incision area was warmed by Ringer's superfusion fluid (35–37°C) (Kraig et al., 1985). DC recordings were made as previously described with a ground electrode placed in temporalis muscle (Kraig et al., 1991; Moskowitz et al., 1993). In selected cases, relative blood flow was measured via a third craniotomy drilled 3 mm anterior to bregma and 2 mm lateral to the midline, leaving the dura intact with an 800-μm probe (P-433-3) and an associated Laserflo™ blood perfusion monitor (model BPM 403; TSI, St. Paul, MN) (Fig. 1).

Hippocampal SD was induced by microinjection of 0.5 M KCl via a glass micropipette with a tip diameter of 4 μm, using pressure pulses of 40 pounds per square inch (psi) for 5–8 s every 9 min over a 2-h period (total of 14 injections) from a Picospritzer-II electronic gas valve system (General Valve; Fairfield, NJ). Recurrent injections (i.e., over 2 h) were used to facilitate c-*fos* expression from SD in the anesthetized animals, since functional activation of c-*fos* immunoreactivity (c-*fos*-IR) tends to reach a maximum after ~1.5 h of stimulation (Bullitt et al., 1992). This is an experimental approach that we have used successfully in the past for measurement of SD-induced changes in expression patterns (Kraig et al., 1991; Caggiano and Kraig, 1996) and is likely to help ensure reproducibility of the challenge (compared with a single SD) (Choudhuri et al., 2002). These investigators also note that no evidence exists to indicate that only one SD accounts for the aura of migraine (and, by extension, to experiments here, potentially noxious stimulation from SD). Recurrent microinjections produced an injection volume of about 10 nl per pulse or <150 nl for the total number of injections, volumes consistent with that seen by other investigators (Stone, 1986). (Injection volume was estimated by injecting 0.5 M KCl from an injection pipette into hydrated light mineral oil and measuring the resultant volume of injectate with a compound microscope calibrated using a stage micrometer.) The injection micropipette was lowered 4.5 mm beneath the neocortical surface into the left hippocampus through the posterior craniotomy (Fig. 1). Sham control animals received analogous microinjections of 0.5 M NaCl. SD, and its absence, were monitored in both the hippocampus and neocortex on the left side with two DC recording microelectrodes, with the shaft of the neocortical recording electrode bent 30 degrees and glued so that its tip was 1.8 mm up the shaft of the hippocampal recording microelectrode. The electrode array was then lowered 2.8 mm beneath the neocortical surface, so that interstitial DC potential could be monitored simultaneously in the neocortex and hippocampus (Fig. 1). Ringer's solution was

applied to the exposed skull surface (1–3 ml/min). Neocortical SD was induced in a similar manner, except that the stimulating electrode was positioned 1 mm beneath the neocortical surface of the posterior craniotomy (Moskowitz et al., 1993). The right side of the brain was always left untouched.

Initially, following the surgical and SD procedures previously described (Moskowitz et al., 1993), c-*fos* immunoreactivity (c-*fos*-IR) in laminae I and II of the TNC was significantly increased over nonsurgical control animals in both SD and sham animals. Accordingly, pilot experiments were conducted that altered the protocol in hopes of reducing c-*fos*-IR in sham control animals toward that found in controls. Protocol changes included (1) increasing the recovery time between craniotomy and SD induction from 7 h to 24 h; (2) changing from lidocaine cream to Bupivacaine; (3) placing eyedrops in the eyes to minimize corneal drying; (4) replacing surgical wound clips with interrupted nylon surgical sutures; (5) replacing the stereotactic frame with a plaster mold to reduce noxious stimulation of the face; and (6) reducing the diameter of the injection pipette. Together, these technical changes reduced the level of c-*fos*-IR in the TNC of neocortical sham and SD animals from previous experiments (Moskowitz et al., 1993) (data not shown). Reduced immunostaining also was evident in the current experiments involving hippocampal SD and sham controls (see below).

Tissue Processing

Immediately after recordings, brains were processed for c-*fos* immunohistochemical staining within the TNC using primary antiserum to c-*fos* (1:10,000; cat. no. sc-52; Santa Cruz Biotechnology, Santa Cruz, CA). The procedures followed those previously described (Nozaki et al., 1992; Caggiano et al., 1996). Frozen coronal sections (40 μm) of the brainstem and spinal cord were sectioned serially through the medulla to the third cervical segment. The obex was used as the most rostral point and was designated 0.0. The first six serial sections from the obex and from regions at 1.5, 3.0, 4.5, and 6.0 mm caudal to the obex were processed and examined in each animal. Forebrain sections were collected 2 mm caudal to bregma. Anatomical boundaries were determined by coordinates established by the Paxinos and Watson (1986) rat brain atlas. Silver intensification of staining was performed according to the procedures of Breder et al. (1992).

Data Analysis and Presentation

TNC c-*fos*-IR cells in the superficial laminae (i.e., I and II) were quantitated as follows. Brain sections were transilluminated using constant illumination through a 540/40-nm bandpass filter (Chroma Technology, Brattleboro, VT) with a X10 objective and X120 overall magnification. Computer-based counting strategies were initially used (Kraig and Kunkler, 1997); however, these counting procedures resulted in undercounting of cells compared with manual methods. Accordingly, c-*fos*-IR cells were counted manually by an observer blinded to experimental conditions, so that all cell counts were done in a random and unbiased fashion. Cells were considered c-*fos*-IR positive if the nucleus was densely stained. Six brain sections were counted at each level of the TNC (i.e., 0, 1.5, 3.0, 4.5, and 6.0 mm caudal to the obex) and the average cell count noted at each level for the left and right sides. Statistical analyses were carried out with Sigma Stat software (version 2.03; SPSS, Chicago, IL). Cell counts were transformed by the square root to stabilize variance (Moskowitz et al., 1993; Snedecor and Cochran, 1989). This permitted pairwise multiple comparisons at all TNC levels (i.e., due to the range of positive cells seen at various TNC levels and in various animal groups). *P*-values of <0.05 were considered significant. All values reported are means ±SEM.

RESULTS

SD and Its Remote Effects

The physiological variables were similar in all experimental groups (Table 1) and were consistent with those of animals anesthetized with halothane and spontaneously breathing (Kraig et al., 1985). As expected, microinjections of KCl in the posterior neocortex for neocortical SD and posterior hippocampus for hippocampal SD induced significantly ($P <$ 0.001) more SDs in hippocampus (11.6 ± 0.5) and neocortex (8.2 ± 0.9) compared with sham controls. More importantly, these injections induced significantly ($P < 0.01$) more SDs in hippocampus than in neocortex.

Neocortical KCl microinjection elicited typical changes of SD throughout the neocortex (Fig. 2). Within 1–2 min of the KCl stimulus, neocortical SD was evident by the large interstitial DC potential change recorded in the parietal neocortex. In addition, blood flow recorded in the frontal neocortex showed characteristic transient elevations in flow with neocortical SD. Blood flow elevations (range, 148–165% of baseline) were significantly greater ($P < 0.001$; n = 5) than those seen with sham controls. Neocortical SD also induced c-*fos*-IR throughout the neocortex. Consistent with previous studies (Moskowitz et al., 1993), neocortical SD did not induce c-*fos*-IR in the hippocampus or subcortical structures. The lack of hippocampal c-*fos*-IR was not unexpected, since the large, negative DC potential change of SD was also absent there after neocortical KCl microinjections. However, subtle electrophysiological changes in the hippocampus accompanied neocortical SD as evidenced by a decrease in spontaneous electrical activity (e.g., thinning of slow DC potential line in upper record, Fig. 2) during neocortical SD. Such thinning of the DC potential line is also seen after cardiac arrest, further supporting the notion that it reflects reduced spontaneous activity.

Likewise, neocortical electrical and blood flow changes were seen with hippocampal SD. Figure 3 shows typical changes from hippocampal SD. Within seconds of the triggering of hippocampal SD, a small negative DC potential change was seen in the neocortex. In addition, spontaneous neocortical electrical activity was transiently diminished. Also, relative neocortical blood flow transiently rose at the onset of hippocampal SD to a level significantly greater than that seen with sham controls (range, 103–125% of baseline; $P = 0.009$; n=5) before returning to baseline. However, the large, interstitial DC potential change observed during neocortical SD was not evident, indicating that hippocampal SD did not propagate to the neocortex. The lack of propagation was further confirmed by the absence of c-*fos*-IR in the neocortex. However, robust immunostaining was evident in the pyramidal and dentate gyrus neurons of the ipsilateral hippocampus.

c-*fos* Protein Response in Caudal Trigeminal Nucleus From Hippocampal SD

c-*fos*-IR cells were found throughout the caudal TNC bilaterally in all groups (Figs. 4-6; Table 2). The appearance of typical immunostained sections 4.5 mm caudal to the obex, the level of maximal change, is shown in Figure 4. Figure 5 displays the typical distribution of c-*fos*-positive immunostaining for all TNC levels and animal groups. Cell counts at all levels and groups (Table 2), transformed by the square root for statistical purposes (Fig. 6), were normally distributed (Kolmogorov-Smirnov test; $P > 0.2$) and passed equal variance tests ($P = 0.01$–0.97). Counts of c-*fos*-IR cells diffusely distributed within laminae I and II fell into two groups: those at 2–4 cells per side/level, and those above this range. In normal animals, c-*fos*-IR cell counts were all within the 2–4 cells per side/level range at each segment. c-*fos*-IR cell counts in both sham and SD animals were also in this low range at segments 0.0 and 1.5 mm. In the more caudal segments, however, differences between experimental groups emerged. Beginning at level 3.0, hippocampal SD induced a robust increase in c-*fos*-IR cell counts that was present bilaterally, but ipsilateral cell counts were always greater than those found

contralaterally. Compared with shams, hippocampal SD induced a significant left, ipsilateral increase in c-*fos*-IR cells ($P = 0.003$) and a similarly significant ($P < 0.001$) contralateral right increase at segment 3.0 mm. At the 4.5-mm segment, the SD-induced significant change was still present bilaterally (ipsilateral, $P<0.001$; contralateral, $P=0.006$) compared with shams, even though sham c-*fos*-IR cell counts were higher than those observed in normal and in more rostral sham segments. However, at the 6.0-mm segment, only the left ipsilateral side remained significantly ($P = 0.04$) greater than sham controls, and overall c-*fos*-IR cell counts declined in both groups compared with segment 4.5 mm. The power of statistical tests with $\alpha = 0.05$ was 0.999–1.000 at segments 3.0, 4.5, and 6.0 mm.

DISCUSSION

The potential interrelation between SD and migraine aura (and subsequent pain; Moskowitz and Macfarlane, 1993; Moskowitz et al., 1993) has been noted since the discovery of SD (e.g., see Leão, 1944; Milner, 1958; Olesen et al., 1981; Andersen et al., 1988; Olesen et al., 1990; Friberg et al., 1994; Lauritzen, 1994; Woods et al., 1994; Welch et al., 1998; Cao et al., 1999; Hadjikhani et al., 2001; James et al., 2001). However, this potential interrelation of SD and migraine aura (or pain) has always involved only neocortical SD. Whether other brain areas susceptible to SD might also be capable of nociceptive activation of the caudal TNC has not been considered. We have begun to remove this void in the present study by showing, for the first time, that the hippocampus is a robust and significant trigger for bilateral TNC nociceptive activation from SD. Furthermore, hippocampal SD can trigger remote blood flow and functional activity changes within the neocortex without spread of SD in that area.

Methodological Considerations

Moskowitz et al. (1993) were the first to develop an animal model showing that neocortical SD (in rodents) was sufficient to activate caudal TNC consistent with what might be expected from migraine pain in humans (Moskowitz and Macfarlane, 1993). Later, Ingvardsen et al. (1998a) were unable to duplicate this result. Unfortunately, numerous methodological differences between these two studies (Moskowitz and Kraig, 1998) precludes meaningful comparison of their results. Ingvardsen et al. (1998b), however, continue to dispute the impact of such differences. It is not our intent, in the present report, to reiterate discussion of differences between these experimental results regarding neocortical SD. Instead, we focus on how changes made in experimental methods in the present investigation (see Materials and Methods) improved the clarity of experimental outcomes compared with the original protocol of Moskowitz et al. (1993) (and thus, also Ingvardsen et al., 1998a, who partially patterned their experiments after Moskowitz et al., 1993).

Effects of the experimental strategy changes can be grouped to two fundamental improvements. The first centers on rostral activation of the caudal TNC. Unlike results of Moskowitz et al. (1993) and presumably Invardsen et al. (1998a), we saw no rostral activation (i.e., levels 0.0 and 1.5 mm). Instead, our results for sham and SD groups were analogous to those for normal animals at these levels. Levels 0.0 and 1.5 of the TNC receive nociceptive input areas that include the snout, tongue, corneas, and eyelids (Strassman and Vos, 1993). Thus, the reduction to normal cell count levels in the rostral segments seen in sham and SD groups probably reflects less stimulation of the involved body parts by our experimental procedures.

The second fundamental difference is the injection volume and tonicity of KCl used to induce SD. Injection volumes designed to faithfully induce hippocampal SD were about 50 times less than that used to faithfully trigger neocortical SD (i.e., 10 nl vs 0.5 μl) (Moskowitz et al., 1993; Ingvardsen et al., 1998a). This finding suggests the heightened susceptibility of hippocampus for SD compared with the neocortex (Bureš et al., 1974) with an efficiency for SD induction of 83% vs 58%, respectively, in the present experiments. Furthermore, concerns

about KCl injections alone triggering activation of TNC via a direct noxious effect to the pial (Ingvardsen et al., 1998a,b) are lessened, as injections were 50-fold smaller and 4.5-fold deeper from the pial surface. It was not feasible to measure potential potassium concentration changes directly at the pial surface above injection sites to confirm this notion. However, we did note that no dye could be seen in that area when examined at X40 stereomicroscopic examination with inclusion of saturated and filtered Fast Green in the injectate. Thus, it is unlikely that KCl injectate drifted to the pial surface in the present experiments. We did not choose to lower the KCl injectate tonicity from 0.5 M to 0.15 M as Moskowitz et al. (1993) did, because this reduction would not allow consistent triggering of SD at our desired, low injectate volumes.

Injectate tonicity may also effect sham results. Injections (nl) of 0.5 M NaCl into the dentate gyrus of anesthetized rats triggers increased apoptosis and subsequent neurogenesis without necrotic injury (Kunkler and Kraig, unpublished observations). We speculate that this may be related to reduced dentate granule cell spontaneous activity from exposure to hypertonic saline, a known effect of hyperosmotic saline on these cells (Sally and Andrew, 1993). Perhaps elevation of c-*fos*-IR in sham controls here includes effects of reduced spontaneous neuronal activity.

Hippocampal SD-Induced Activation of TNC

Hippocampal SD significantly activated the caudal TNC in a pattern similar to that seen from neocortical SD (Moskowitz et al., 1993) and consistent with studies involving nociceptive activation of TNC from pial and meningeal trigeminal afferents (for review see Mitsikostas and Sanchez del Rio, 2001). Indeed, c-*fos*-IR activation of the superficial laminae of the TNC via various noxious meningeal and nervous system stimuli (i.e., SD) are used as a rodent/feline model of vascular headache in humans (Mitsikostas and Sanchez del Rio, 2001). For example, chemical activation after meningeal irritation by blood (Nozaki et al., 1992) and mechanical stimulation of dural blood vessels (Strassman et al., 1994) leads to increased c-*fos*-IR mainly in laminae I and II and I and V, respectively. Noxious chemical and mechanical stimulation of the meninges in rats also leads to increased c-*fos*-IR primarily in lamina I and II (Malick et al., 2001). In contrast, using electrophysiological measures of TNC cell activation, Ebersberger et al. (2001) were unable to show that neocortical SD could trigger heightened activity in the TNC. However, these investigators recorded from cells within the deeper laminae of the TNC that were identified by initial activation to mechanical stimulation of the dura, instead of the more superficial cells (i.e., found in laminae I and II) known (as noted above) to be sensitive to mechanical stimuli of dural blood vessels (Strassman et al., 1994; Malick et al., 2001).

Bilateral activation of caudal TNC from unilateral hippocampal SD may stem from the commissural connections associating both sides of the hippocampus (Swanson and Cowan, 1977; Schwartzkroin and McIntyre, 1988). For example, although unilateral hippocampal SD does not propagate to the contralateral side (Kunkler and Kraig, unpublished observations), activation of the contralateral TNC may stem from associated altered spontaneous activity. The following conclusion stems from evidence that SD can trigger synaptically remote changes in blood flow, spontaneous activity, and gene expression (Kraig et al., 1991; Caggiano and Kraig, 1996).

The mechanisms by which hippocampal SD triggers nociceptive activation of TNC are undefined, just as they remain for neocortical SD (Moskowitz et al., 1993). Furthermore, similar to efferent pathways from neocortex (Moskowitz et al., 1993), no connections are obvious from hippocampus whereby SD in that area could activate the TNC via a synaptic circuit. Instead, it seems likely that, as suggested for neocortex (Moskowitz et al., 1993), hippocampal SD might trigger nociceptive activation of the TNC via diffusion of noxious substances from neural cells through the interstitial space and to trigeminal afferents in the pia. These afferents are concentrated at the base of the brain, including the point where the

hippocampus reaches the pial surface (Moskowitz, 1990). Perhaps, neocortical functional changes and changes in cerebral blood flow from hippocampal SD contribute to dura-based trigeminal afferent nociceptive activation.

Further support for the notion of pial irritation from SD comes from the work of Bolay et al. (2002). This work provides strong evidence potentially linking migraine aura and headache by showing that neocortical SD activates trigeminovascular afferents and evokes cortical meningeal and brainstem changes consistent with the development of headache. Similar effects may account for hippocampal SD induction of increased c-*fos*-IR in the superficial laminae of the TNC since the hippocampus also reaches the pial surface. However, Koroleva and Bureš (1993) contest the suggestion that SD can be noxious in an investigation showing that neither neocortical nor hippocampal SD induced aversive behavior in rats. Altered behavior can be an important measure of noxious stimuli from visceral pain (Ness et al., 1991). Nonetheless, the perception of pain is made complex by aspects of mentation that include attention, understanding, control expectations, mood, and the aversive significance of the noxious stimulus (McGrath, 1994). Our experiments described in the present report were not designed to determine whether hippocampal SD is necessarily perceived as painful. Instead, we sought to demonstrate that hippocampal SD could be a noxious stimulus consistent with what might be seen with migraine, which might help stimulate further study of vascular headache in animals and humans centering on the role of SD in the hippocampus.

Neocortical SD in humans has been notoriously difficult to demonstrate by classical electrophysiological criteria. While noted after severe head trauma in humans (Mayevsky et al., 1996), it has never been shown in association with migraine. In contrast, slowly propagating changes in blood flow have been noted using the Xenon-133 technique (Lauritzen et al., 1983; Andersen et al., 1983; Olesen et al., 1981, 1990), functional MRI (fMRI) technology (Friberg et al., 1994; Welch et al., 1998; Cao et al., 1999; Hadjikhani et al., 2001), and positron emission tomography (PET) scanning (Woods et al., 1994; Weiller et al., 1995). Using the latter technology, Woods et al. (1994) showed that a propagating neocortical hypoperfusion can occur during a migraine attack (without aura). In this case, the blood flow reduction was interpreted to start in Brodmann's areas 18 and 19. However, close inspection of the primary data (i.e., Fig. 2, top, second image from right; Woods et al., 1994) shows that the medial temporal lobe also is an initial site for the hypoperfusion though spreading of the hypoperfusion within the hippocampus has not been specifically examined to date. Furthermore, Weiller et al. (1995) used PET technology to demonstrate brainstem activation (i.e., increased blood flow) during migraine attacks. Data from this latter report also show blood flow changes within the temporal lobe. Although these changes are not the most robust noted, they do provide further support for involvement of the hippocampus in migraine. Finally, work by Horowitz et al. (1968) provides additional support for this notion. These investigators noted that electrical stimulation of the posterior hippocampus in patients could produce visual distortions of actual perceptions, elementary visual sensations (e.g., colored lights, geometric forms and amorphous shapes, and so-called "externally placed" visual hallucinations). Thus, it is conceivable that hippocampal SD not only can activate TNC, but potentially might contribute to remote functional changes elsewhere, such as neocortex. Our findings of neocortical blood flow and electrophysiological changes remote from hippocampal SD begin to suggest this possibility for future detailed study.

Hadjikhani et al. (2001) provide convincing indirect evidence that a neocortical SD-like phenomenon can be a concomitant of migraine aura. Our results show, for the first time, that another brain area, the hippocampus, may also be important in the pathogenesis of migraine. This conclusion takes on added impact with consideration of the recent work by Calandre et al. (2002). These investigators showed that interictal disturbances in memory of migraineurs, which are proportional to the frequency of their attacks or the longevity of their migraine

history, involve both sides of the hippocampus. Thus, both animal and human studies begin to suggest that further study of hippocampus may be important in deciphering the pathogenesis of migraine.

Acknowledgments

REFERENCES

Andersen AR, Friberg L, Olsen T Skyhøj, Olesen J. Delayed hyperemia following hypoperfusion in classic migraine. Arch. Neurol 1988;45:154–159. [PubMed: 3257687]

Avoli M, Drapeau C, Louvel J, Pumain R, Olivier A, Villemure JG. Epileptiform activity induced by low extracellular magnesium in the human cortex maintained in vitro. Ann Neurol 1991;30:589–596. [PubMed: 1686384]

Bolay H, Reuter U, Dunn AK, Huang Z, Boas DA, Moskowitz MA. Intrinsic brain activity triggers trigeminal meningeal afferents in a migraine model. Nat Med 2002;8:136–142. [PubMed: 11821897]

Breder CD, Smith WL, Raz A, Masferrer J, Seibert K, Needlemman P, Saper CB. The distribution and characterization of cyclooxygenase-like immunoreactivity in the ovine brain. J Comp Neurol 1992;322:409–438. [PubMed: 1517485]

Bullitt E, Chong LL, Light AR, Willcockson H. The effect of stimulus duration on noxious-stimulus induced c-*fos* expression in the rodent spinal cord. Brain Res 1992;580:172–179. [PubMed: 1504797]

Bureš, J.; Burešová, O.; Křivánek, J. The mechanism and applications of Leão's spreading depression of electroencephalographic activity. Academic Press; San Diego, CA: 1974.

Caggiano AO, Kraig RP. Eicosanoids and nitric oxide influence induction of reactive gliosis from spreading depression in microglia but not astrocytes. J Comp Neurol 1996;369:93–108. [PubMed: 8723705]

Caggiano AO, Breder CB, Kraig RP. Long-term elevation of cyclooxygenase-2, but not lipoxygenase, in regions synaptically distant from spreading depression. J Comp Neurol 1996;376:447–462. [PubMed: 8956110]

Cajal, SR. General structure of the cerebral cortex. In: Swanson, N.; Swanson, LW., translators. Histology of the nervous system. Vol. Vol. 2. Oxford University Press; New York: 1995. p. 429-492.

Calandre EP, Bembibre J, Arnedo ML, Becerra D. Cognitive disturbances and regional cerebral blood flow abnormalities in migraine patients: their relationship with clinical manifestations of illness. Cephalgia 2002;22:291–302.

Cao Y, Welch KMA, Aurora S, Vikingstad EM. Functional MRI-BOLD of visually triggered headache in patients with migraine. Arch Neurol 1999;56:548–554. [PubMed: 10328249]

Choudhuri R, Lisa C, Yong C, Bowyer S, Klein RM, Welch KMA, Berman NEJ. Cortical spreading depression and gene regulation: relevance to migraine. Ann Neurol 2002;51:499–506. [PubMed: 11921056]

Cutrer, M.; Waeber, M.; Moskowitz, M. Headaches. In: Joynt, RJ.; Griggs, RC., editors. Baker's clinical neurology [CD-ROM]. Lippincott/Williams & Wilkins; Philadelphia: 2001.

Ebersberger A, Schaible H-G, Averbeck B, Richter F. Is there a correlation between spreading depression, neurogenic inflammation, and nociception that might cause migraine headache? Ann Neurol 2001;49:7–12. [PubMed: 11198299]

Ferrari M. Migraine. Lancet 1998;351:1043–1051. [PubMed: 9546526]

Friberg L, Olesen J, Lassen NA, Olsen T Skyhøj, Karle A. Cerebral oxygen extraction, oxygen consumption, and regional cerebral blood flow during the aura phase of migraine. Stroke 1994;25:974–979. [PubMed: 8165693]

Grafstein B. Mechanism of spreading cortical depression. J Neurophysiol 1956;19:154–171. [PubMed: 13295838]

Hadjikhani N, Sanchez del Rio M, Wu O, Schwartz D, Bakker D, Fischl B, Kwong KK, Cutrer FM, Rosen BR, Tootell RBH, Sorensen AG, Moskowitz MA. Mechanisms of migraine aura revealed by functional MRI in human visual cortex. Proc Natl Acad Sci U S A 2001;98:4687–4692. [PubMed: 11287655]

Horowitz MJ, Adams JE, Rutkin BB. Visual imagery on brain stimulation. Arch Gen Psychiatry 1968;19:469–486. [PubMed: 4876804]

Ingvardsen BK, Laursen H, Olsen UB, Hansen AJ. Possible mechanism of c-*fos* expression in trigeminal nucleus caudalis following cortical spreading depression. Pain 1998a;72:407–415. [PubMed: 9313281]

Ingvardsen BK, Laursen H, Olsen UB, Hansen AJ. Letter to the editor. Pain 1998b;76:266–267.

James MF, Smith JM, Boniface SJ, Huang CL, Leslie RA. Cortical spreading depression and migraine: new insights from imaging? Trends Neurosci 2001;24:266–271. [PubMed: 11311378]

Koroleva VI, Bureš J. Rats do not experience cortical or hippocampal spreading depression as aversive. Neurosci Lett 1993;149:153–156. [PubMed: 8474690]

Kraig RP, Kunkler PE. Hippocampal spreading depression may trigger migraine pain. Ann Neurol 1997;42:445.

Kraig RP, Pulsinelli WA, Plum F. Hydrogen ion buffering in brain during complete ischemia. Brain Res 1985;342:181–290.

Kraig RP, Dong L, Thisted L, Jaeger CB. Spreading depression increases immunohistochemical staining of glial fibrillary acidic protein. J Neurosci 1991;11:2187–2198. [PubMed: 1906091]

Lashley KS. Patterns of cerebral integration indicated by the scotomas of migraine. Arch Neurol Psychiatry 1941;46:331–339.

Lauritzen M. Pathophysiology of the migraine aura: the spreading depression theory. Brain 1994;117:199–210. [PubMed: 7908596]

Lauritzen M, Olsen T Skyhøj, Lassen NA, Paulson OB. Changes in regional cerebral blood flow during the course of classic migraine attacks. Ann Neurol 1983;13:633–641. [PubMed: 6881926]

Leão AAP. Spreading depression of activity in the cerebral cortex. J Neurophysiol 1944;7:359–390.

McGrath PA. Psychological aspects of pain perception. Archs Oral Biol 1994;39(suppl):55S–62S.

Malick A, Jakubowski M, Elmquist JK, Saper CB, Burstein R. A neurochemical blueprint for pain-induced loss of appetite. Proc Natl Acad Sci U S A 2001;98:9930–9935. [PubMed: 11504950]

Marshall WH. Spreading cortical depression of Leão. Physiol Rev 1959;39:239–279. [PubMed: 13645235]

Mayberg MR, Langer RS, Zervas NT, Moskowitz MA. Perivascular meningeal projections from cat trigeminal ganglia: possible pathway for vascular headache in man. Science 1981;213:228–230. [PubMed: 6166046]

Mayberg MR, Zervas NT, Moskowitz MA. Trigeminal projections to supratentorial pial and dural blood vessels in cats demonstrated by horseradish peroxidase histochemistry. J Comp Neurol 1984;223:46–56. [PubMed: 6200513]

Mayevsky A, Doron A, Manor T, Meilin S, Zarchin N, Ouaknine GE. Cortical spreading depression recorded from the human brain using a multiparametric monitoring system. Brain Res 1996;740:268–274. [PubMed: 8973824]

Menetrey D, Basbaum AI. The distribution of substance P-enkephalin- and dynorphin-immunoreactive neurons in the medulla of the rat and their contribution to bulbospinal pathways. Neuroscience 1987;23:173–187. [PubMed: 2446203]

Milner PM. Note on possible correspondence between the scotomas of migraine and spreading depression of Leão. EEG Clin Neurophysiol 1958;10:705.

Mitsikostas DD, Sanchez del Rio M. Receptor systems mediating c-*fos* expression within trigeminal nucleus caudalis in animal models of migraine. Brain Res Rev 2001;35:20–35. [PubMed: 11245884]

Moskowitz MA. Basic mechanisms in vascular headache. Neurol Clin 1990;8:801–815. [PubMed: 2175382]

Moskowitz MA, Macfarlane R. Neurovascular and molecular mechanisms in migraine headaches. Cerebrovasc Brain Metab Rev 1993;5:159–177. [PubMed: 8217498]

Moskowitz MA, Kraig RP. Letter to the editor. Pain 1998;76:265–271. [PubMed: 9696482]

Moskowitz MA, Nozaki K, Kraig RP. Neocortical spreading depression provokes the expression of c-*fos* protein-like immunoreactivity within the trigeminal nucleus caudalis via trigeminovascular mechanisms. J Neurosci 1993;13:1167–1177. [PubMed: 8382735]

Ness TJ, Randich A, Gebhart GF. Further behavioral evidence that colorectal distension is a noxious visceral stimulus in rats. Neurosci Lett 1991;131:113–116. [PubMed: 1791969]

Nozaki K, Boccalini P, Moskowitz MA. Expression of c-*fos*-like immunoreactivity in brainstem after meningeal irritation by blood in the subarachnoid space. Neuroscience 1992;49:669–680. [PubMed: 1501769]

Olesen J, Larsen B, Lauritzen M. Focal hyperemia followed by spreading oligemia and impaired activation of rCBF in classic migraine. Ann Neurol 1981;9:344–352. [PubMed: 6784664]

Olesen J, Friberg L, Olsen T Skyhøj, Iversen HK, Lassen NA, Andersen AR, Karle A. Timing and topography of cerebral blood flow aura, and headache during migraine attacks. Ann Neurol 1990;28:791–798. [PubMed: 2285266]

Paxinos, G.; Watson, C. The rat brain in stereotaxic coordinates. Academic Press; San Diego, CA: 1986.

Sally V, Andrew RD. CA3 neuron excitation and epileptiform discharge are sensitive to osmolality. J Neurophysiol 1993;69:2200–2208. [PubMed: 8350139]

Schwartzkroin, PA.; McIntyre, Dc. Limbic anatomy and physiology. In: Engel, T.; Pedley, T., editors. Epilepsy, a comprehensive textbook. Lippincott-Raven; Philadelphia: 1998. p. 323-340.

Snedecor, GW.; Cochran, WG. Statistical methods. Iowa State University Press; Ames, IA: 1989. p. 107-130.

Stone, TW. Microiontophoresis and pressure ejection. John Wiley & Sons; New York: 1986. The release of compounds from micropipettes and the tissue concentrations achieved; p. 39-75.

Šramka M, Brožek G, Bureš J, Nádvorník P. Functional ablation by spreading depression: possible use in human stereotaxic neurosurgery. Appl Neurophysiol 197778;40:48–61.

Strassman AM, Mineta Y, Vos BP. Distribution and fos-like immunoreactivity in the medullary and upper cervical dorsal horn produced by stimulation of dural blood vessels in the rat. J Neurosci 1994;14:3725–3735. [PubMed: 8207485]

Strassman AM, Vos BP. Somatotopic and laminar organization of fos-like immunoreactivity in the medullary and upper cervical dorsal horn induced by noxious facial stimulation in the rat. J Comp Neurol 1993;331:495–516. [PubMed: 8509507]

Sugaya E, Yakato M, Noda Y. Neuronal and glial activity during spreading depression in cerebral cortex of cat. J Neurophysiol 1975;38:822–841. [PubMed: 1159468]

Swanson LW, Cowan WM. An autoradiographic study of the organization of the efferent connections of the hippocampal formation in the rat. J Comp Neurol 1997;172:49–84. [PubMed: 65364]

Weiller C, May A, Limmroth V, Juptner M, Kaube H, Schayck RV, Coenen HH, Diener HC. Brain stem activation in spontaneous human migraine attacks. Nat Med 1995;1:658–660. [PubMed: 7585147]

Welch KMA, Cao Y, Aurora S, Wiggins G, Vikingstad EM. MRI of the occipital cortex, red nucleus, and substantia nigra during visual aura of migraine. Neurology 1998;51:1465–1469. [PubMed: 9818884]

Woods RP, Iacoboni M, Mazziotta JC. Bilateral spreading cerebral hypoperfusion during spontaneous migraine headache. N Engl J Med 1994;331:1689–1692. [PubMed: 7969360]
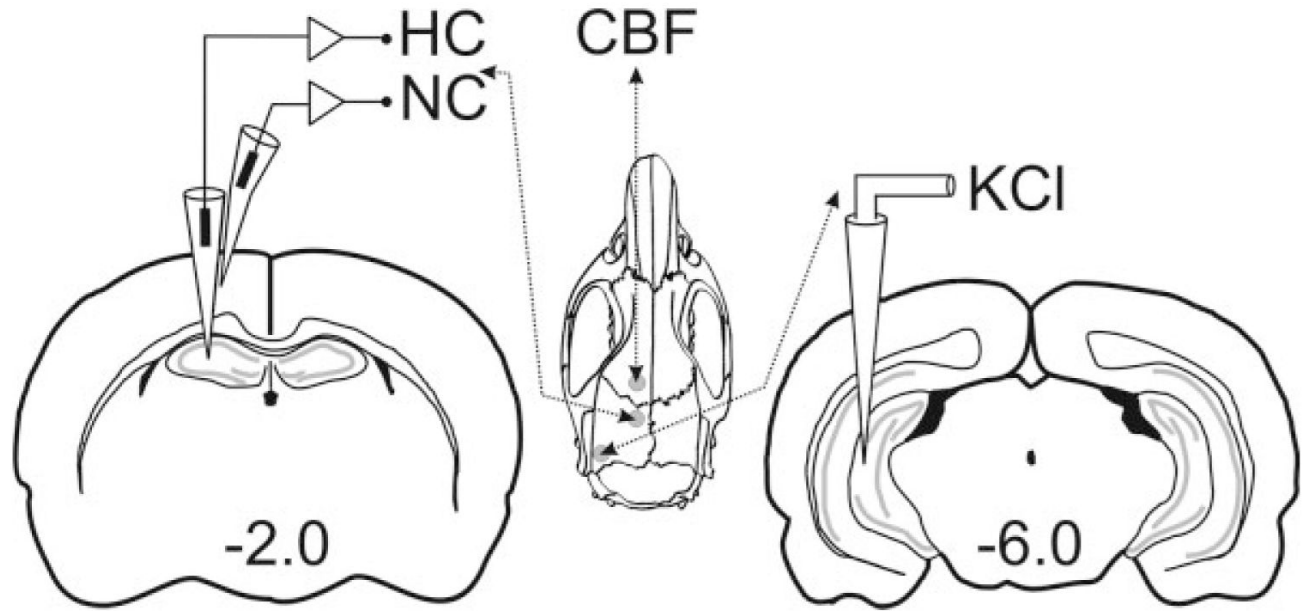
FIGURE 1.
Schematic of experimental method. Center image shows rat skull with gray circles depicting sites of craniotomies. DC recordings were made through one of two craniotomies made in all animal groups (−2.0 mm from bregma and 1.5 mm lateral to the midline). Two microelectrodes glued together were passed through this craniotomy so that the deeper microelectrode was 2,800 μm below the pial surface in the hippocampus (HC), while at the same time the second microelectrode was positioned 1,000 μm into the neocortex (NC) (image to left). Spreading depression (SD) was induced by a microelectrode passed through the posterior craniotomy (−6.0 mm from bregma and 4.5 mm lateral to the midline) and lowered to a depth of 4,500 μm below the pial surface for hippocampal SD (image to the right) or 1,000 μm below the pial surface for induction of neocortical SD. In selected instances a third craniotomy was drilled over the frontal cortex (3 mm anterior to bregma and 2.0 mm lateral to the midline) to measure relative cerebral blood flow (CBF).
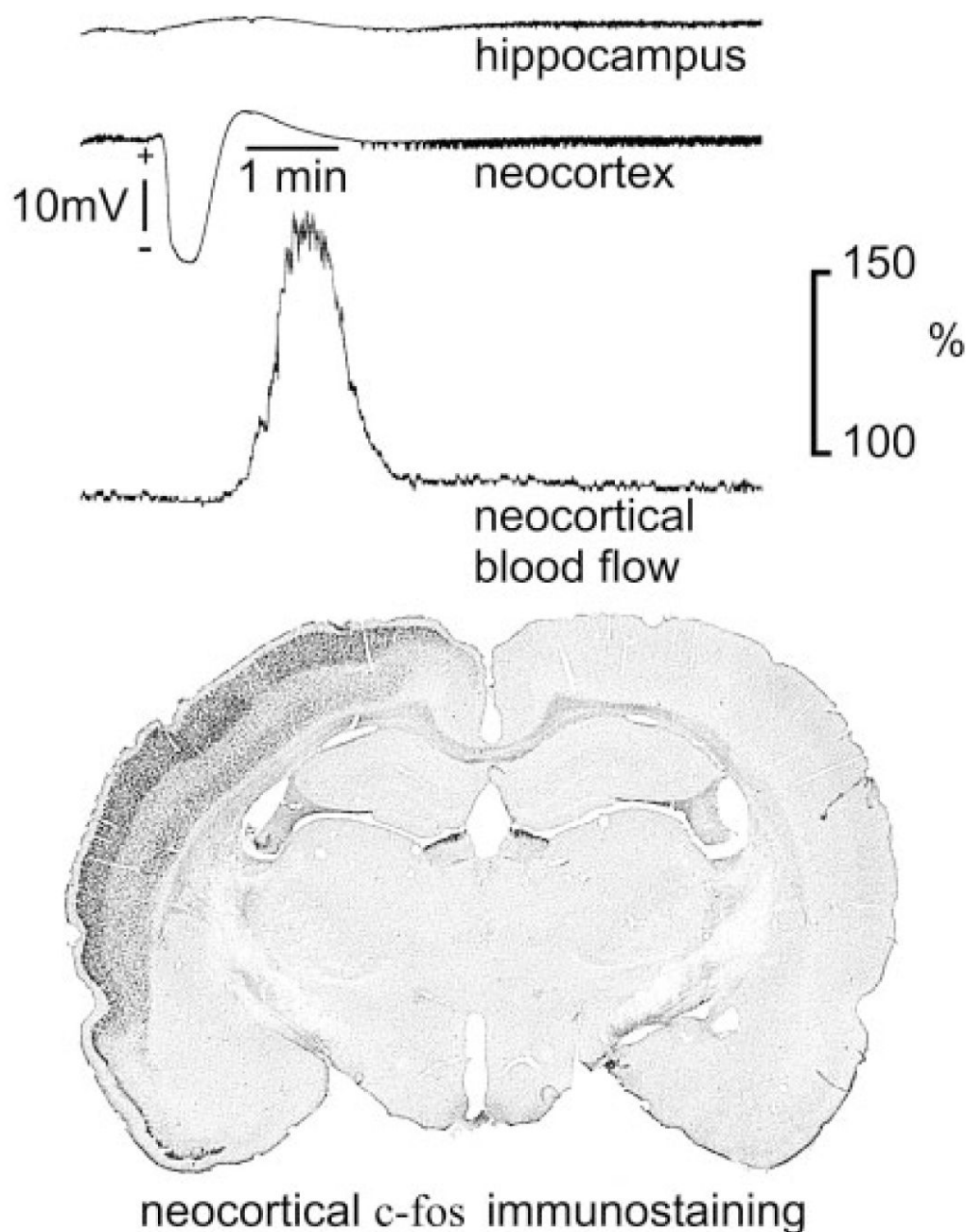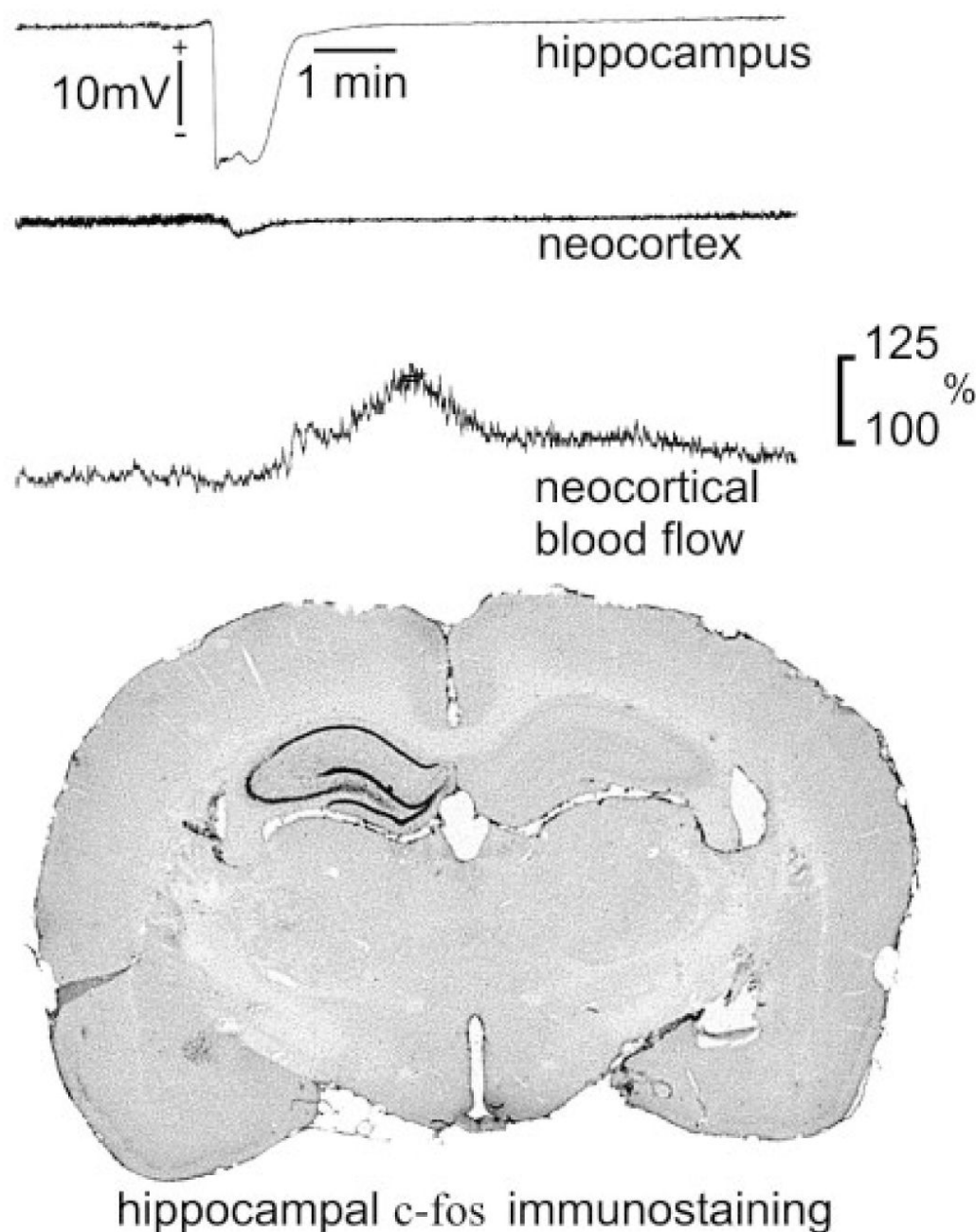
FIGURE 2.
Responses to neocortical spreading depression (SD). Microinjections of 0.5 M KCl (stimulus point not shown) into posterior neocortex were used to trigger neocortical SD. Typical changes are shown. Neocortical interstitial DC potential changes showed the typical electrophysiological changes of SD (middle record). A large negative DC potential change was preceded and followed by smaller positive DC changes. Furthermore, spontaneous electrical activity (shown by small negative-going DC changes, which thicken the neocortical DC record) was lost during SD. Neocortical SD did not propagate to hippocampus (top record), but muted DC changes occurred in the form of a positive-going small, slow DC change shortly after the neocortical DC change of SD reached its zenith. Also, spontaneous electrical activity

transiently diminished but progressively returned in hippocampus comparable to the return in neocortex after SD. Consistent with previous reports, SD induced a transient rise in blood flow during neocortical SD to more than 150% of initial baseline level (established before recurrent SDs were induced; range, 148–165% of baseline; n=5). The delay between blood flow and DC change results from the caudal to rostral propagation of SD, which reaches the DC recording site before moving on the blood flow recording site. Blood flow in the record shown begins from below 100% because SD also causes a more protracted reduction in blood flow and the record shown is from the 6th of 14 induced SD. Bottom image shows associated c-*fos* immunoreactivity (c-*fos*-IR) changes after recurrent neocortical SD (elicited every 9 min for 2 h). Dense c-*fos*-IR was restricted to the ipsilateral neocortex which experienced SD.
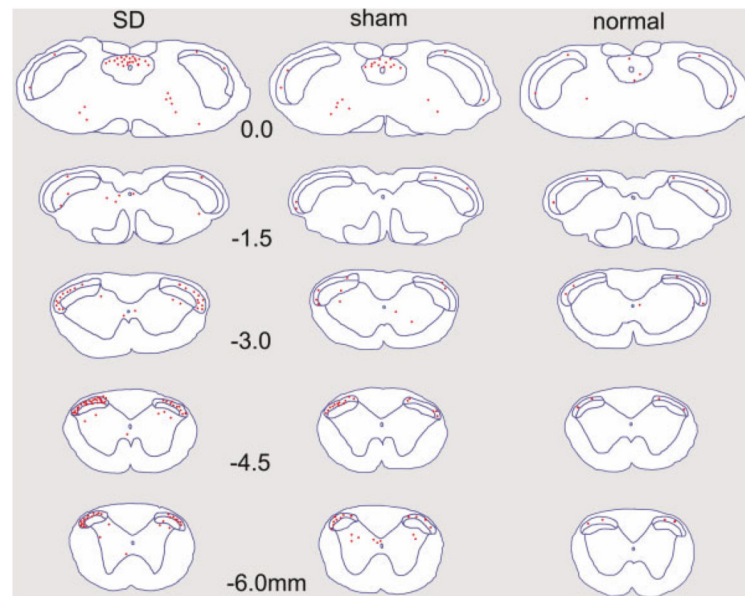
FIGURE 3.
Responses to hippocampal spreading depression (SD). Microinjections of 0.5 M KCl (stimulus not shown) into posterior hippocampus were used to trigger hippocampal SD. Typical changes are shown. After 1–2 min, interstitial DC potential changes of SD were evident in rostral hippocampus (top record). Large interstitial, negative potential change occurred with a transient cessation of spontaneous electrical activity (i.e., narrowing of DC record during SD and a progressive thickening near the end of the record shown). Electrophysiological changes of SD did not extend into the neocortex (middle record), yet electrophysiological changes did occur in that area. Hippocampal SD induced a small negative-going shift in the neocortical DC potential and reduced spontaneous neocortical electrical activity during and for minutes after

hippocampal SD. In addition, neocortical blood flow rose to 125% (range, 103–125% of baseline; n = 5) of control (i.e., blood flow level before the first SD with the 8th of 14 hippocampal SDs shown). The DC recordings are from microelectrodes placed in the same vertical axis centered in parietal cortex while the blood flow measurements were made from frontal cortex. The cause for the temporal disparity between DC and blood flow records is unknown. Bottom image shows c-*fos* immunoreactivity (c-*fos*-IR) immediately after recurrent hippocampal SD (elicited every 9 min for 2 h). c-*fos*-IR is observed in the pyramidal cell layer and dentate gyrus of the ipsilateral hippocampus, but not in neocortex or contralateral hippocampus.
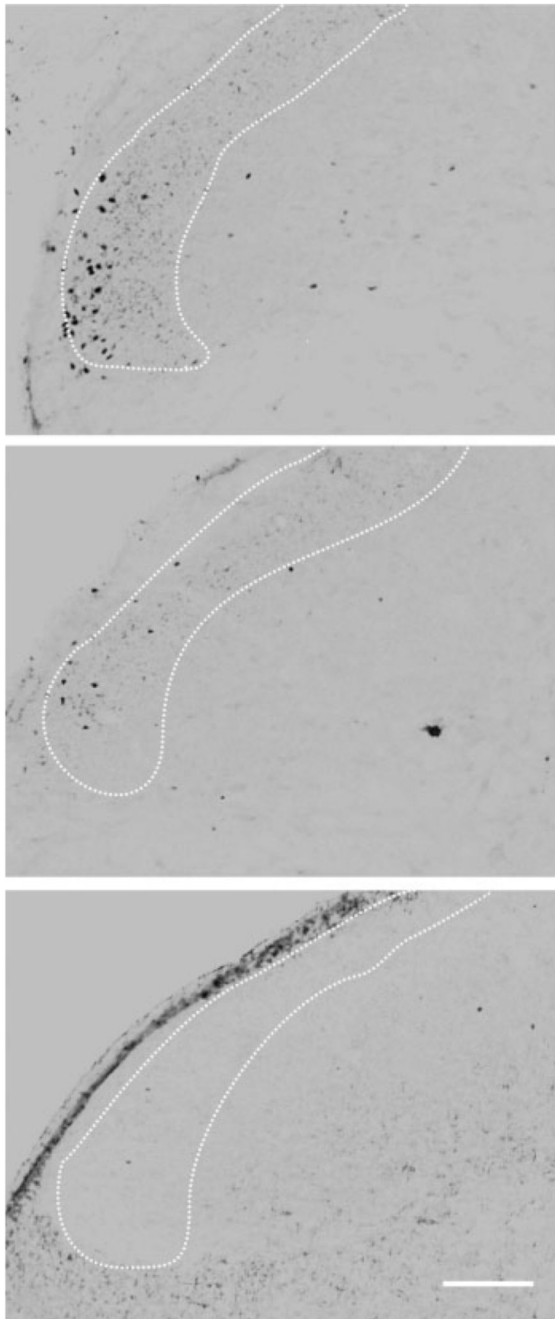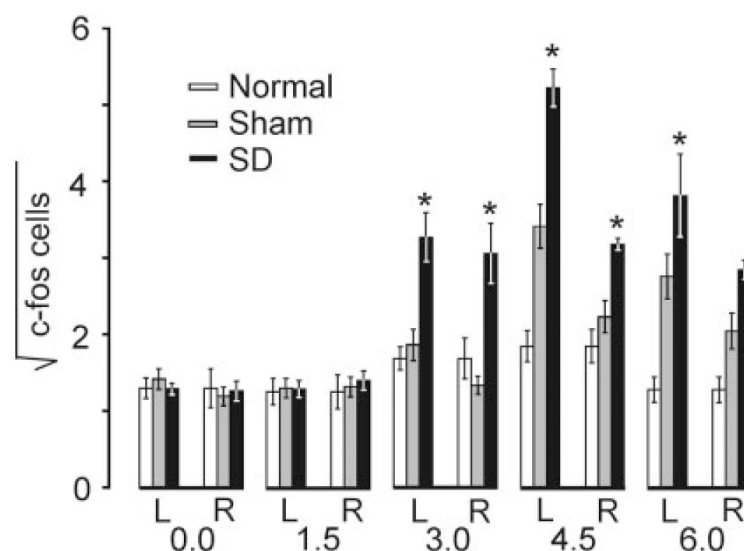
FIGURE 4.
Staining patterns for c-*fos* immunoreactivity (c-*fos*-IR) of the trigeminal nucleus (TNC). Images shown are from sections 4.5 mm caudal to the obex, the TNC level of maximal c-*fos*-IR change. Manual counting procedures were aided by silver intensification, which tended to blacken c-*fos*-IR-positive cells, and visualization through a 540/40 bandpass filter, which reduced background. Dotted lines encircle laminae I and II for the TNC from representative hippocampal spreading depression (SD) (top), sham control (middle), and normal (bottom) animal groups. Top image shows 26 positive cells; middle image, 8 positive cells; and bottom image, no cells that would be considered positive within encircled area used for quantification. Scale bar = 100 μm.

FIGURE 5.
Anatomic distribution of c-*fos* immunoreactivity (c-*fos*-IR) cells in the trigeminal nucleus (TNC) after hippocampal spreading depression (SD). Camera lucida drawings of c-*fos*-IR in the medulla and C1 of the rat spinal cord emphasize the effect of hippocampal SD on TNC activation. Each dot represents a c-*fos*-IR cell. Hippocampal SD, triggered every 9 min for 2 h in the caudal hippocampus, induced bilateral TNC c-*fos*-IR. c-*fos*-IR cells in lamina I–II of the TNC were primarily found near C1 with increased induction observed at 3.0, 4.5, and 6.0 mm and normal levels seen more rostrally at 0.0 and 1.5 mm. Sham operated controls, which received microinjections of 0.5 M NaCl, displayed a similar pattern of c-*fos*-IR but labeled significantly fewer cells ($P < 0.05$– 0.001) at 3.0, 4.5, and 6.0 mm. Sporadic c-*fos*-IR cells were present throughout the TNC of normal animals but at levels that were never significantly different from sham and experimental group levels at 0.0 and 1.5 mm.

FIGURE 6.
Quantification of c-*fos* immunoreactivity (c-*fos*-IR) cell counts in the trigeminal nucleus (TNC) after hippocampal spreading depression (SD). Cell counts were transformed by the square root to stabilize variance and permit simultaneous comparison of all experimental groups, levels, and sides measured. All experimental groups showed analogous levels of laminae I and II c-*fos*-IR at rostral TNC levels (i.e., 0 and 1.5 mm). These levels receive nociceptive input from areas that include snout, tongue, cornea, and eye lids. On the other hand, sham and experimental animals showed a similar pattern of c-*fos* activation within laminae I and II of the TNC bilaterally at levels 3.0, 4.5, and 6.0 mm. In each instance SD induced an ipsilateral, left (*) increase in c-*fos*-IR compared with sham controls that reached significance levels (*) of $P < 0.003$ at 3.0, $P < 0.001$ at 4.5, and P 0.04 at 6.0 mm. Without traveling to the contralateral, right hippocampus, SD induced a right-sided caudal TNC c-*fos* activation compared with sham controls that reached significance levels of $P < 0.001$ at 3.0 and 0.006 at 4.5 mm.

TABLE 1

Physiologic Variables and Number of SD[†]

Group	pH	PaCO$_2$ (torr)	PaO$_2$ (torr)	Hematocrit (%)	Temperature (°C)	Glucose (mM)	SD
Hippocampal SD	7.29 ± 0.01	61 ± 2	100 ± 5	41 ± 0	37.0 ± 0.2	4.4 ± 0.1	11.6 ± 0.5[*,**]
Neocortical SD	7.29 ± 0.01	62 ± 2	93 ± 3	42 ± 0	37.0 ± 0.1	4.2 ± 0.2	8.2 ± 0.9[*]
Sham	7.28 ± 0.02	62 ± 2	92 ± 3	42 ± 0	37.0 ± 0.1	4.2 ± 0.3	0

SD, spreading depression.

[†] Data are means ±SEM with n = 5 per group.

[*] $P < 0.001$ for hippocampal and neocortical SD compared with sham controls.

[**] $P < 0.01$ for hippocampal SD compared with neocortical SD.

TABLE 2

c-fos-Positive Cell Counts Within the Trigeminal Nucleus[*]

Level (mm)	Normal		Hippocampal sham		Hippocampal SD	
	Left	Right	Left	Right	Left	Right
0	1.7 ± 0.4	1.9 ± 0.8	2.1 ± 0.4	1.5 ± 0.3	1.7 ± 0.2	1.7 ± 0.3
1.5	3.0 ± 0.6	1.8 ± 0.7	1.7 ± 0.3	1.8 ± 0.3	1.7 ± 0.3	2.0 ± 0.4
3.0	3.0 ± 0.5	3.1 ± 0.9	3.6 ± 0.8	1.8 ± 0.3	11.1 ± 2.1	10.0 ± 2.5
4.5	3.5 ± 0.8	3.6 ± 0.8	12.0 ± 1.9	5.2 ± 0.9	27.5 ± 2.6	10.1 ± 0.5
6.0	2.2 ± 0.5	1.7 ± 0.4	7.9 ± 1.6	4.4 ± 1.0	15.7 ± 4.1	8.2 ± 0.7

SD, spreading depression.

[*] Data are means ±SEM derived from six histological sections per level and five animals per group.